

Finite element analysis of concrete cracking at early age

Mauren Aurich*¹, Américo Campos Filho^{2a}, Túlio Nogueira Bittencourt^{3a} and Surendra P. Shah^{4a}

¹Department of Civil Engineering, Pontifical Catholic University of Rio Grande do Sul, Brazil

²Department of Civil Engineering, Federal University of Rio Grande do Sul, Brazil

³Polytechnical School, University of São Paulo, Brazil

⁴Department of Civil Engineering, Northwestern University, Evanston, IL, USA

(Received June 18, 2009, Accepted October 21, 2010)

Abstract. The study of the early age concrete properties is becoming more important, as the thermal effects and the shrinkage, even in the first hours, could generate cracks, increasing the permeability of the structure and being able to induce problems of durability and functionality in the same ones. The detailed study of the stresses development during the construction process can be decisive to keep low the cracking levels. In this work a computational model, based on the finite element method, was implemented to simulate the early age concrete behavior and, specially, the evaluation of the cracking risk. The finite element analysis encloses the computational modeling of the following phenomena: chemical, thermal, moisture diffusion and mechanical which occur at the first days after the concrete cast. The developed software results were compared with experimental values found in the literature, demonstrating an excellent approach for all the implemented analysis.

Keywords: concrete; early age; thermal analysis; moisture transport; mechanical analysis.

1. Introduction

The study of the concrete properties evolution at the early age is becoming increasingly important, as the release of the cement hydration heat and the concrete shrinkage in the first hours, could generate cracks, increasing the permeability of the structure and inducing durability and functionality problems in the same ones. Indeed, there is a limited understanding of the concrete behavior at early age and doubts on the usual applied models validity. A detailed study of the stresses evolution during this period can be decisive to maintain low levels of cracking.

The finite element analysis can provide an accurate evaluation of the concrete behavior at early age. The possibility of coupling the shrinkage and thermal effects, both dependent on the boundary conditions and the materials properties, makes the application of the finite element method an economic and technically appropriate tool, to replace the usual design methods.

Although the development of numerous software using the finite element method has spread out

*Corresponding author, Professor, E-mail: maurenaurich@gmail.com

^aProfessor

this technique, it is demanded an adequacy of these programs to incorporate of the main transient factors related to concrete shrinkage and deformation at first ages. To validate the modeling, the computational results shall be compared with experimental results. Thus, a better understanding of the concrete behavior at early age and a tool to predict the concrete cracking in these ages are obtained.

The aim of this study is to develop strategies for computational modeling of the following phenomena: chemical, heat, moisture diffusion and mechanical, that comprise the concrete history at early age, for a better interpretation of the experimental results and stress states evaluation, aiming to foresee the concrete cracking. In the chemical analysis, the heat generated by exothermic reactions of cement hydration is evaluated. In the thermal analysis, the program also considers the heat flow due to the temperature difference between body and environment. The nodal temperatures are determined considering the thermal and geometrical properties. Subsequently, the moisture diffusion analysis is performed. Considering the analogy between the heat transfer and moisture diffusion equations, the same procedures of thermal analysis are employed to evaluate the nodal values of relative pore humidity. The mechanical analysis calculates the stress states due to temperature and humidity values evaluated in previous steps, and due to concrete shrinkage and creep. When the stress state of a sample point reaches the failure surface, it is considered cracked.

So, it is necessary, initially, the study of the appropriate constitutive laws to model concrete hydration, shrinkage and cracking. Then, techniques for modeling will be discussed and simulations performed, to compare with experimental results already carried through by other researchers, to validate the implemented software. After the modeling validation, it is intended to interpret consistently experimental results available in literature and from other software.

Over the past several years, many numerical tools have been developed to evaluate the measures adopted to reduce the cracking risk at early age (Aurich 2008, Lura 2000, Morabito 1998, Shah *et al.* 1997). These tools are based on mathematical models capable to describe the coupling of thermal, moisture diffusion, chemical and mechanical analysis.

In this work, a methodology for evaluate the potential cracking risk in concrete structures at early age is described. It will be shown numerical models to describe the main aspects of the chemical, thermal, moisture diffusion and mechanical phenomena that occur during the first days after the concrete cast and a computational implementation of these models through the finite element method.

2. Chemical analysis

The analysis of the concrete behavior at early age requires the knowledge of the processes involved in chemical reactions, as well as in the subsequent development of the physical properties at macroscopic level. The addition of water causes the beginning of the cement hydration reaction. The hydration process is responsible for the paste microstructure formation and consequent development of the concrete mechanical properties.

However, the chemical reactions associated with the cement hydration have a remarkably exothermal character with strong heat release, generating a volumetric expansion and, after that, a contraction. The presence of internal or external constraints may lead to concrete cracking.

In this analysis, the heat released due to the exothermic reactions of the cement hydration is determined by a concrete adiabatic temperature rise curve. In this study, the curve proposed by the

Japan Society of Civil Engineers (JSCE) or a curve determined from experimental data could be used.

According to JSCE, the adiabatic temperature value, during the hydration reactions development, can be estimated according to Eq. (1).

$$\theta_{\text{adiab}} = \theta_{\text{max}}(1 - e^{1,25 \cdot t}) \quad (1)$$

where, θ_{max} is the maximum temperature achieved by cement in the calorimetric test and t is time, expressed in days (between 0 and 70 days).

This analysis generates a volumetric load, in a perfect analogy with the structure self-weight, but instead of a force, it generates heat. This heat released due to the temperature rise inside the body is the input for the next step, the thermal analysis.

3. Thermal analysis

The heat transfer is the movement of thermal energy due to temperature differences. Thus, when temperature differences occur in an environment, or between different bodies, there are conditions for the heat transfer. In the study of concrete at early age, the heat transfer can occur by two ways: conduction and convection of the air at the concrete surface.

According with Bathe (1996) for a heat transfer analysis in a two-dimensional body, assuming that the material obeys the Fourier's Law of heat conduction, it can be written that

$$q_x = -k_x \frac{\partial \theta}{\partial x} \quad q_y = -k_y \frac{\partial \theta}{\partial y} \quad (2)$$

where q_x and q_y are heat flows conducted per unit area, θ is the body temperature and, k_x and k_y are thermal conductivities corresponding to the principal axes x , y .

Considering the heat flow equilibrium inside the body, it is obtained that

$$\frac{\partial}{\partial x} \left(k_x \frac{\partial \theta}{\partial x} \right) + \frac{\partial}{\partial y} \left(k_y \frac{\partial \theta}{\partial y} \right) = -q^B \quad (3)$$

where q^B is the rate of heat generated per unit volume.

On the surface of the body, the following conditions must be satisfied

$$\theta|_{S_\theta} = \theta^S \quad (4)$$

$$k_n \frac{\partial \theta}{\partial n} \Big|_{S_q} = q^S \quad (5)$$

where θ^S is the known temperature at the surface S_θ , k_n is the thermal conductivity of the body, \mathbf{n} is the unit normal vector to the surface of the body and q^S is the prescribed heat flux input on the body surface S_q .

Three boundary conditions may be considered in the heat transfer analysis:

√ Temperature conditions: the temperature may be prescribed or fixed on certain points or surfaces of the body, denoted by S_θ in Eq. (4);

- √ Heat flow conditions: the heat flow input may be prescribed in certain points or surfaces of the body. These heat flow boundary conditions S_q are specified in Eq. (5);
- √ Convection boundary conditions: the convection may be included as boundary condition, adding the following term in Eq. (5)

$$q^S = h(\theta_e - \theta^S) \quad (6)$$

where h is the convection coefficient. Here at environmental temperature θ_e is known, but the surface temperature θ^S is unknown.

For the finite element solution of the heat transfer problem, using the principle of virtual temperatures, given as

$$\int_V \bar{\theta}'^T k \theta' dV = \int_V \bar{\theta} q^B dV + \int_{S_q} \bar{\theta}^S q^S dS + \sum_i \bar{\theta}^i Q^i \quad (7)$$

where,

$$\theta'^T = \left[\frac{\partial \theta}{\partial x} \quad \frac{\partial \theta}{\partial y} \right], \text{ and } T \text{ denotes the transposed vector} \quad (8)$$

$$k = \begin{bmatrix} k_x & 0 \\ 0 & k_y \end{bmatrix} \quad (9)$$

and Q^i is the concentrated heat flow input. Each Q^i is equivalent to a surface heat flow, over a very small area. The bar over the temperature θ indicates that a virtual temperature distribution is being considered.

In the heat transfer problem considered above only it is assumed steady state conditions. However, when significant heat flow input changes are specified over a short time period (due to a change of any boundary conditions or the heat generation in the body), it is important to include a term that takes account of the rate at which heat is stored within the material. The rate of heat absorption may be considered as

$$q^c = \rho c \dot{\theta} \quad (10)$$

where c is the material specific heat capacity. The variable q^c can be understood as a part of the heat generated, which must be subtracted from the otherwise generated heat q^B in the Eq. (7). This effect leads to a transient response solution.

4. Moisture diffusion analysis

Since Bazant and Najjar (1972), studies had always shown that the correct prediction of the moisture diffusion in concrete structures is extremely important. Current studies (Kwon and Shah 2008, Baluch *et al.* 2008) attest that the solution of this problem is essential to evaluate the stress states due to shrinkage, creep and thermal expansion. Also, the pore humidity directly affects the mechanical strength, the thermal conductivity and the cement degree of hydration.

In the diffusion most general case, according to Kwon and Shah (2008) and Jeon (2008), gases,

liquids and solutions are transported, through a porous medium, according with the Fick's First Law of Diffusion, considering a transient phenomenon, such as drying of the concrete, the balance equation is given by

$$\frac{\partial H}{\partial t} = \frac{\partial}{\partial x} \left(D(H) \frac{\partial H}{\partial x} \right) \quad (11)$$

where $D(H)$ is the diffusion coefficient (m^2/s) at relative pore humidity H and dH/dx is the gradient in relative pore humidity (m^{-1}).

A study conducted by Baluch *et al.* (2008) utilized the analogy between the heat transfer analysis and the moisture diffusion inside of a concrete body. Using the analogy, the differential equation that governs the heat transfer phenomenon, in the transient solution, can be written as

$$\frac{\partial \theta}{\partial t} = \frac{k}{\rho c} \left(\frac{\partial^2 \theta}{\partial x^2} + \frac{\partial^2 \theta}{\partial y^2} \right) \quad (12)$$

where $\theta = \theta(x, y, t)$ is the temperature as a function of location variables x and y and the time variable t , k is the thermal conductivity, c is specific heat, and ρ is density.

Similarly, rewriting the differential equation that governs the moisture diffusion phenomenon, it is transformed to

$$\frac{\partial H}{\partial t} = D(H) \left(\frac{\partial^2 H}{\partial x^2} + \frac{\partial^2 H}{\partial y^2} \right) \quad (13)$$

where $H = H(x, y, t)$ is the pore relative humidity as a function location variables x and y and the time variable t , and $D(H)$ is the moisture diffusion coefficient (usually as a function of H).

Considering the boundary conditions in the heat transfer analysis, it can be written that

$$\frac{\partial \theta}{\partial n} = h(\theta_e - \theta^S) \quad (14)$$

where $\partial \theta / \partial n$ is the thermal gradient at the surface, h is the convective coefficient, θ_e is the environmental temperature and θ^S is the surface temperature.

Also, considering the boundary conditions in the moisture diffusion analysis, it can be written that

$$D(H) \frac{\partial H}{\partial n} = \alpha_m (H_e - H^S) \quad (15)$$

Table 1 Corresponding terms in the differential equations for moisture diffusion and heat transfer (Baluch 2008)

| Heat transfer | | Moisture diffusion |
|--------------------|-------------------|--------------------|
| $\theta(x, y, t)$ | \leftrightarrow | $H(x, y, t)$ |
| $\frac{k}{\rho c}$ | \leftrightarrow | $D(H)$ |
| h | \leftrightarrow | α_m |
| θ_e | \leftrightarrow | H_e |
| θ^S | \leftrightarrow | H^S |

where $\partial H/\partial n$ is the moisture gradient at the surface, α_m is the mass transfer factor, H_e is the relative pore humidity at the surface of the porous medium and H^s is the relative humidity of the ambient space.

Comparing the equations that describe the moisture diffusion and heat transfer analysis, it is clear that exists an analogy between both problems. The correspondence between the parameters in the analyses can be seen in Table 1.

5. Mechanical analysis

Finite elements for axis-symmetrical, plane stress and strain analyses have been implemented. The concrete is represented through a viscoelastic model, corresponding to a chain composed by five Maxwell's elements in parallel. It was presented by Bazant and Wu (1974) an algorithm to automatically determinate the parameters $E_\mu(t)$ and $\eta_\mu(t)$ for each age, t of concrete, from experimental results or standard concrete values. According to Aurich (2008) this model is calibrated from the creep formulation presented in CEB-FIP Model Code 1990 (1993) or *fib* (1999).

The concrete shrinkage and thermal expansion strains are considered as prescribed deformations on structure. As creep, concrete shrinkage strains are evaluated according to CEB-FIP Model Code 1990 (1993) or *fib* (1999), which considers different expressions to determinate the autogenous and the drying shrinkage.

The failure criterion proposed by Ottosen (1997) is adopted to identify concrete cracking. This failure criterion was adopted by CEB-FIP Model Code 1990 (1993) and is expressed by

$$\alpha \frac{J_2}{f_{cm}^2} + \lambda \frac{\sqrt{J_2}}{f_{cm}} + \beta \frac{I_1}{f_{cm}} - 1 = 0 \quad (16)$$

where f_{cm} is the mean value of concrete compressive strength and

$$\begin{aligned} \lambda &= c_1 \cos[1/3 \arccos(-c_2 \sin 3\phi)], \quad \text{for } \sin 3\phi \leq 0 \\ \lambda &= c_1 \cos[\pi/3 - 1/3 \arccos(c_2 \sin 3\phi)], \quad \text{for } \sin 3\phi > 0 \end{aligned} \quad (17)$$

$$\sin 3\phi = -\frac{3\sqrt{3} J_3}{2 J_2^{3/2}} \quad (18)$$

and I_1 is the first invariant of stress tensor, J_2 , J_3 are the second and the third invariant of deviatoric stress tensor.

The concrete stress-strain behavior of concrete subjected to tensile stresses should be expressed by two relations: a stress-strain relationship representing the behavior of the concrete outside the fracture zone and a stress-crack opening relation which describes the deformations occurring within the fracture zone.

To represent the uncracked concrete behavior, subjected to tension, CEB-FIP Model Code 1990 (1993) suggests a bilinear stress-strain relationship, as given in Eq. (19) and Eq. (20).

$$\begin{aligned} \sqrt{\quad} & \quad \text{for } \sigma \leq 0,9f_{cm} \\ \sigma_{ct} &= E_c \cdot \varepsilon_{ct} \end{aligned} \quad (19)$$

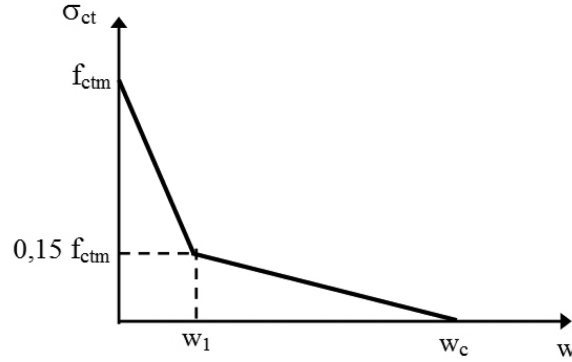


Fig. 1 Stress-crack opening diagram for cracked concrete

$$\sqrt{\quad} \quad \text{for } 0,9f_{ctm} \leq \sigma_{ct} \leq f_{ctm}$$

$$\sigma_{ct} = f_{ctm} - \frac{0,1f_{ctm}}{0,00015 - \frac{0,9f_{ctm}}{E_c}} (0,00015 - \varepsilon_{ct}) \quad (20)$$

where E_c is the tangent modulus of elasticity, f_{ctm} is the tensile strength, σ_{ct} is the tensile stress and ε_{ct} is the tensile strain.

The CEB-FIP Model Code 1990 (1993) also presents for a cracked section a stress-crack opening diagram, as shown in Fig. 1.

Eq. (21) to Eq. (24) describe the bilinear stress-crack opening relationship, which evaluates strain in cracked concrete.

$$\sqrt{\quad} \quad \text{for } 0,15f_{ctm} \leq \sigma_{ct} \leq f_{ctm}$$

$$\sigma_{ct} = f_{ctm} \left(1 - 0,85 \frac{w}{w_1} \right) \quad (21)$$

$$\sqrt{\quad} \quad \text{for } 0 \leq \sigma_{ct} \leq 0,15f_{ctm}$$

$$\sigma_{ct} = \frac{0,15f_{ctm}}{w_c - w_1} (w_c - w) \quad (22)$$

and

$$w_1 = 2 \frac{G_F}{f_{ctm}} - 0,15w_c \quad (23)$$

$$w_c = \beta_F \frac{G_F}{f_{ctm}} \quad (24)$$

where w_1 is the crack opening, w_c is the crack opening for $\sigma_{ct} = 0$, G_F is the fracture energy and β_F is the coefficient that depends on the maximum aggregate size as given in Table 2.

Table 2 Coefficients α_F and β_F

| d_{max} (mm) | α_F | β_F |
|----------------|------------|-----------|
| 8 | 0.02 | 8 |
| 16 | 0.03 | 7 |
| 32 | 0.05 | 5 |

The fracture energy, G_F , can be calculated as

$$G_F = \alpha_F \left(\frac{f_{cm}}{10} \right)^{0.7} \tag{25}$$

where α_F is a coefficient that depends on the maximum aggregate size, also given in Table 2.

6. Numerical applications

Numerical applications of the described methodologies throughout this work are presented in this item.

6.1 Concrete rings

A test using a ring specimen to study the concrete cracking with restrained shrinkage was developed by Grzybowski and Shah (1990). The test consists in a concrete ring internally limited by a steel ring, in which are placed strain-gages for strain measuring, and an external microscope to measure the crack width. The tests proposed by the authors were conducted at ACBM laboratory (Center for Advanced Cement-Based Materials at Northwestern University, Evanston, Illinois), with the purpose to compare different types of shrinkage-reducing admixtures performances at early age. The dimensions of the specimens are given in Fig. 2.

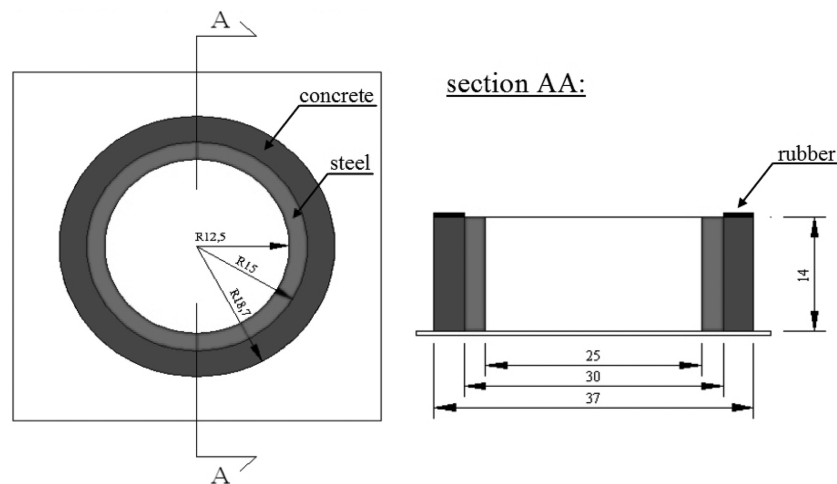


Fig. 2 Dimension (cm) of the ring test specimen



Fig. 3 Concrete ring framework and steel rings, the strain-gages position and the prepared ring specimen placed in environmental chamber

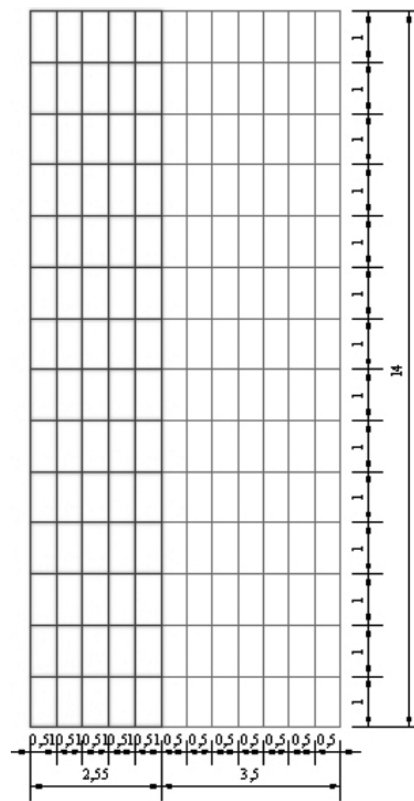


Fig. 4 Finite element mesh

The specimens were cured for 4 hours at 20°C and 100% RH, and then after demolding exposed to drying in the humidity room at the ambient temperature of 20°C and 40% RH.

Fig. 3 illustrates the test, the position of the strain-gages in the steel rings and concrete ring prepared for testing.

To analysis the algorithm results, this work studies two rings (Shah *et al.* 1993, 1997). Aurich (2008) developed a parametric study to determine the mesh refinement required to obtain accurate results. The mesh used for the rings finite element analysis has 168 elements and can be seen in Fig. 4.

Table 3 Materials properties

| Properties | Concrete | Steel |
|--|----------------------------------|--------------------|
| Thermal conductivity (kJ/cm.day.°C) | 2.33 | 45.55 |
| Convection coefficient (kJ/cm ² .day.°C) | 0.12 | – |
| Thermal capacity (kJ/cm ³ .day) | 1.16 | 0.419 |
| Diffusion coefficient (m ² /s) | 0.06048 | 1.10 ⁻⁹ |
| Mass transfer factor | 3.33 | – |
| Young modulus (kN/cm ²) | 2500 (ring 1) 3500 (ring 2) | 20000 |
| Poisson ratio | 0.2 | 0.3 |
| Compressive strength (28 days) (kN/cm ²) | 3.034 (ring 1) 3.556 (ring 2) | – |

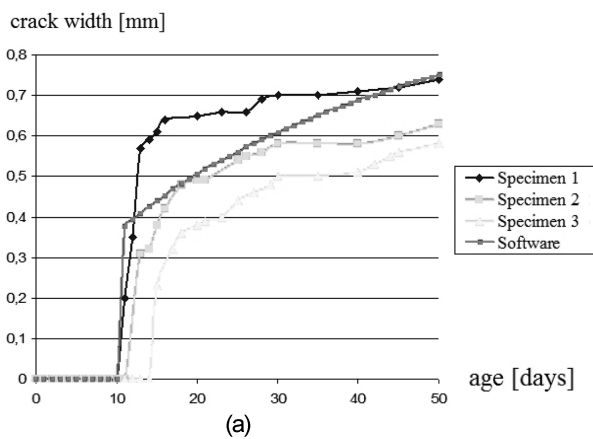


Fig. 5(a) Crack width (ring 1)

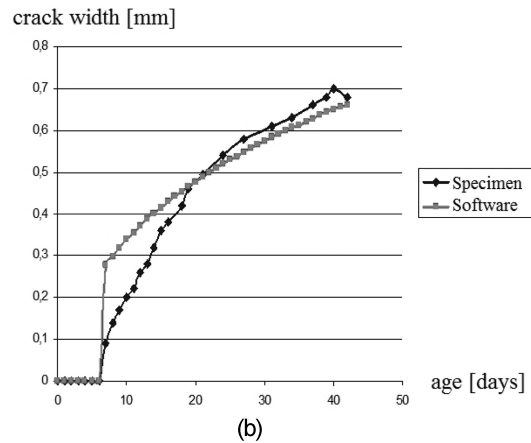


Fig. 5(b) Crack width (ring 2)

The parameters considered in the thermal, moisture diffusion and mechanical analysis for both studied rings are shown in Table 3.

Fig. 5(a) shows the comparison between the numerical and experimental results for the time at which the cracks occur and the increase of the crack opening for ring 1 (Shah *et al.* 1997). The Fig. 5(b) presents the same comparison for ring 2 (Shah *et al.* 1993). In the mechanical analysis, the crack widths were evaluated using the stress-crack opening diagram showed in Fig. 1.

6.2 Concrete prisms

A uniaxial test using a dog bone specimen was developed by Kvoler (1994) to analyze the concrete cracking with restrained shrinkage. The fundamental idea of the test was to measure the stress until the time of cracking under temperature and humidity controlled conditions.

The measurements had been carried only through in the body of the prism, throughout a length of 62.23 cm. The cross section of the extremities was gradually increased to fit in the test mechanism

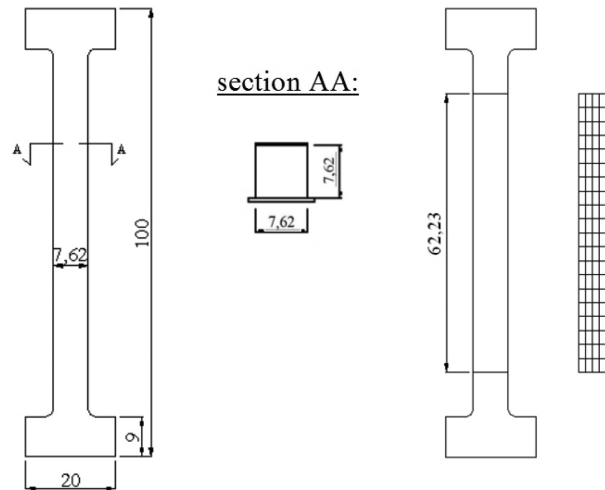


Fig. 6 Specimen dimension (cm) and finite element mesh

Table 4 Concrete properties

| Properties | Concrete |
|--|----------------------------------|
| Thermal conductivity (kJ/cm.day.°C) | 2.33 |
| Convection coefficient (kJ/cm ² .day.°C) | 0.12 |
| Thermal capacity (kJ/cm ³ .day) | 1.16 |
| Diffusion coefficient (m ² /s) | 0,06048 |
| Mass transfer factor | 3.33 |
| Young modulus (kN/cm ²) | 3500 (prism 1) 2500 (prism 2) |
| Poisson ratio | 0,2 |
| Compressive strength (28 days) (kN/cm ²) | 2.80 (prism 1) 2.10 (prism 2) |

and minimizes the stress concentration in those areas. The top and the bottom surfaces were sealed to allow symmetrical drying from the other two sides of the specimen. With these boundary conditions a two dimensional analysis is sufficient to simulate the test.

This paper studies two concrete prisms tested by Altoubat and Lange (2001), and presents the comparison between experimental and numerical results for the shrinkage stress and the age of cracking.

The dimensions of the tested prism and the finite element mesh are presented in Fig. 6. Table 4 shows the materials properties considered in the analyses.

The tensile stresses developed in both restrained samples and the algorithm results are shown in Fig. 7(a) and Fig. 7(b).

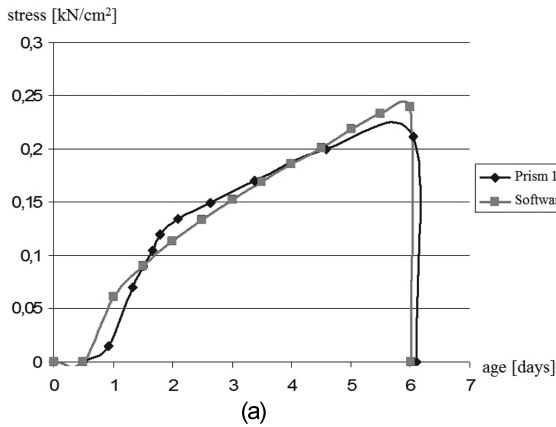


Fig. 7(a) Normal stresses (prism 1)

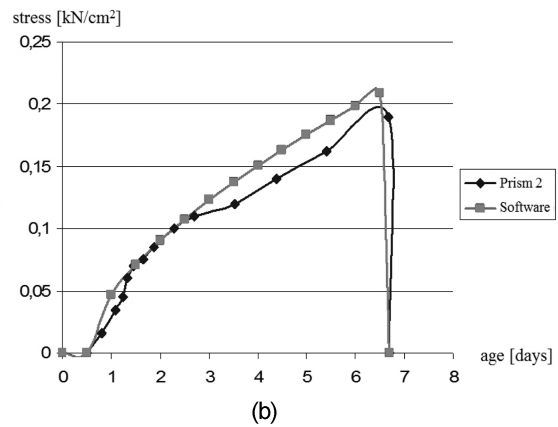


Fig. 7(b) Normal stresses (prism 2)

6.3 Tetrapod

The tetrapod is a component used as a cover element for a breakwater protection, consisting of a single block of concrete composed of four axisymmetric cone legs. It can reach heights in order of 4 meters with the maximum diameter of the legs of 2 meters.

To analyze this kind of element, this paper studied the tetrapod examined by de Borst and van den Boogaard (1994). A finite element mesh of 165 elements, as seen in Fig. 8, was used in the analyses. And, the materials properties are listed in Table 5.

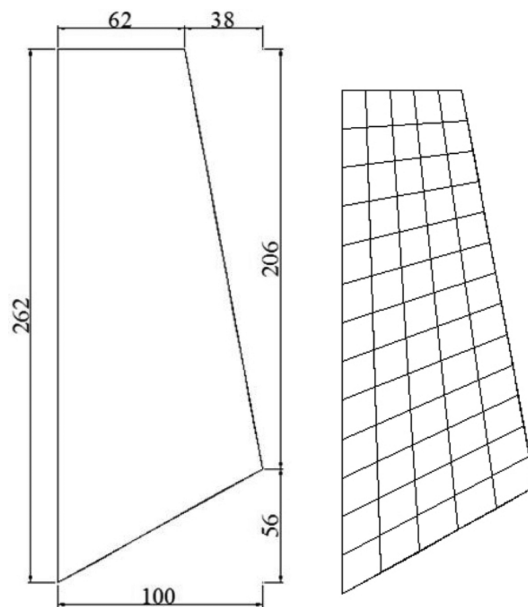


Fig. 8 Finite element mesh

Table 5 Concrete properties

| Properties | Concrete |
|--|----------|
| Thermal conductivity (kJ/cm.day.°C) | 2.33 |
| Convection coefficient (kJ/cm ² .day.°C) | 0.12 |
| Thermal capacity (kJ/cm ³ .day) | 1.16 |
| Diffusion coefficient (m ² /s) | 0,06048 |
| Mass transfer factor | 3.33 |
| Young modulus (kN/cm ²) | 2700 |
| Poisson ratio | 0,2 |
| Compressive strength (28 days) (kN/cm ²) | 2.50 |

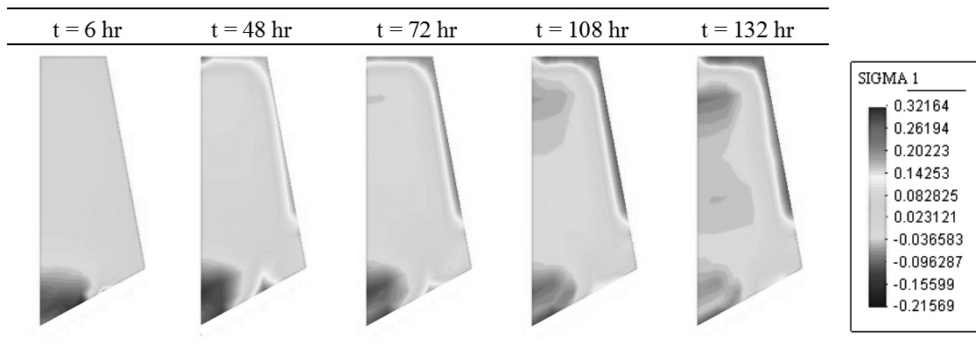


Fig. 9 Principal stresses maps (kN/cm²)



Fig. 10 Cracked tetrapod

The evolution maps of the tensile stresses are shown in Fig. 9. It is important to observe that, according to the finite element analysis, the higher tensile stress value appears on the tetrapod surface, generating cracks in these regions, confirming what was actually observed, according to Fig. 10.

7. Conclusions

This work presents a computational model, based on the finite element method, to simulate the concrete behavior at early age. The finite element analysis encloses the computational modeling of the chemical, thermal, diffusion and mechanical phenomena, which occur during the first days after the concrete cast.

The results of the computational modeling are compared with experimental values from literature, demonstrating an excellent approximation at all solution stages.

At first the behavior of the ring-type specimens in restrained shrinkage cracking tests were simulated by the implemented software. The experimental results for the time at which the cracks occur and the increase of the crack opening, obtained by [4, 16], were compared to the software results. The analysis values and the tests data were very close.

In the second example dog bone specimen for a uniaxial restrained shrinkage tests, performed by [18], were analyzed. The comparisons between experimental and numerical results showed an accurate agreement.

Finally the early age behavior of a concrete tetrapod was examined. The tetrapod is a component used as a cover element for a breakwater protection, consisting of a single block of concrete composed of four axisymmetric cone legs. Considering the temperature rising due to the heat generated by the cement hydration and the moisture diffusion inside the body, the software demonstrated capacity to predict the crack formation at the tetrapod surface.

The results achieved, even considering the concrete behavior inherent variability, demonstrated that the adopted models could simulate the actual concrete behavior at early age. The implemented finite element model proved to be an accurate and appropriate tool to predict the concrete cracking in different concrete structures.

Acknowledgements

This research project was supported by the Brazilian National Council for Scientific and Technological Development (CNPq), by the Coordination of Improvement of Higher Education (CAPES), and by Center for Advanced Cement-Based Materials at Northwestern University (ACBM).

References

- Altoubat, S.A. and Lange, D.A. (2001), "Creep, shrinkage and cracking of restrained concrete at early age", *ACI Mater. J.*, **98**(4), 323-331.
- Aurich, M. (2008), "Numerical simulation of the early age concrete behavior", Ph.D. Dissertation, Polytechnical School at University of São Paulo.
- Baluch, M.H., Rahman, M.K. and Mahmoud, I.A. (2008), "Calculating drying-shrinkage stresses", *Concrete Int. Mag.*, **30**(7), 37-41.
- Bathe, K.J. (1996), *Finite Element Procedures*, Englewood Cliffs, New Jersey, Prentice Hall.
- Bazant, Z.P. and Najjar, L.J. (1972), "Nonlinear water diffusion in nonsaturated concrete", *Mater. Struct.*, **5**(1), 3-20.
- Bazant, Z.P. and Wu, S.T. (1974), "Rate-type creep law of aging concrete based on maxwell chain", *Mater.*

- Struct.*, **7**(1), 45-60.
- Comité Euro-International du Béton (1993), *CEB-FIP Model Code 1990*, Bulletin d'Information, 213/214.
- de Borst, R. and van den Boogaard, A.H. (1994), "Finite-element modeling of deformation and cracking in early-age concrete", *J. Eng. Mech.-ASCE*, **120**(12), 2519-2534.
- Fédération Internationale du Béton (1999), *Structural Concrete*, Textbook on Behavior, Design and Performance - Updated Knowledge of the CEB/FIP Model Code 1990, (Bulletin 1-3).
- Grzybowski, M. and Shah, S.P. (1990), "Shrinkage cracking of fiber reinforced concrete", *J. Am. Concrete Inst.*, **87**(2), 138-148.
- Jeon, S.J. (2008), "Advanced assessment of cracking due to heat of hydration and internal restraint", *ACI Mater. J.*, **105**(4), 325-333.
- Kvolder, K. (1994), "Testing system for determining the mechanical behavior of early age concrete under restrained and free uniaxial shrinkage", *Mater. Struct.*, **27**(34), 324-330.
- Kwon, S.H. and Shah, S.P. (2008), "Prediction of Early Age Cracking of Fiber-Reinforced Concrete Due to Restrained Shrinkage", *ACI Mater. J.*, **105**(4), 381-389.
- Lura, P. (2000), "Autogenous deformation and internal curing of concrete", Ph.D. Dissertation, Delft University of Technology, Delft.
- Morabito, P. (1998), *Methods to Determine the Heat of Hydration of Concrete. Prevention of Thermal Cracking in Concrete at Early Ages*, Report 15, R. Springenschmid, E & FN SPON.
- Ottosen, N.S. (1997), "A failure criterion for concrete", *J. Eng. Mech. Div.-ASCE*, **103**(4), 527-535.
- Shah, S.P., Karaguler, M.E. and Sarigaphuti, M. (1993), "Effects of Shrinkage-Reducing Admixtures on Restrained Shrinkage Cracking of Concrete", *ACI Mater. J.*, **89**(3), 138-148.
- Shah, S.P., Ouyang, C., Marikunte, S., Yang, W. and Aldea, C. (1997), "Control of cracking with shrinkage-reducing admixtures", *Transp. Res. Rec.*, **1574**, 25-36.